Pulse Duration Dependence of Novel Metal Alloying on Fe/Cr/Ni Thin Films by Ultra-Short Pulsed Laser Irradiation

Taiyoh Kawano[1], Taketo Furuichi[1], Eibon Tsuchiya[2], Makoto Yamaguchi[3],
Tatsuya Okada[1], Yohei Kobayashi[2], and Takuro Tomita[*1]

[1]*Graduate School of Science and Technology for Innovation, Tokushima University, Japan*
[2]*Institute for Solid State Physics, University of Tokyo, Japan*
[3]*Graduate School of Engineering Science, Akita University, Japan*
[*]*Corresponding author's e-mail: tomita@tokushima-u.ac.jp*

We examined the possibility of suppressing elemental segregation of high-entropy alloys (HEAs) using femtosecond laser irradiation. Thin films of iron (Fe), chromium (Cr), and nickel (Ni) were deposited on the surfaces of n-type SiC and p-type GaN substrates. The thicknesses of the Fe, Cr, and Ni films were 12, 7, and 11 nm, respectively. Laser irradiation was performed from the substrate side by focusing on the interface between the Fe film and substrate. Scanning transmission electron microscopy (STEM) bright-field images superimposed on the elemental maps of Fe, Cr, and Ni showed a more homogenous mixing of Fe, Cr, and Ni in the femtosecond-laser-modified region than in the picosecond-laser-modified region. In particular, the Ni distribution showed a significant improvement in homogeneity. In other words, the Ni mixture was more homogeneous in the femtosecond laser-modified region than in the picosecond laser-modified region. Although the duration of the picosecond laser pulse was sufficiently long for atomic diffusion, segregation still occurred during the cooling process following laser irradiation.

1. Introduction

Ultrashort pulsed laser processing has attracted considerable attention from both fundamental and practical perspectives [1-6]. In addition to the cutting of materials, an ultrashort pulsed laser can be used to modify the material properties of the irradiated area. The density, absorption coefficient, and refractive index can be modified by irradiating the focal spot with an ultrashort pulsed laser beam. During the ultrashort pulsed laser-induced modification process, it is assumed that the thermal trajectories induced by ultrashort pulsed laser irradiation are different from those induced by nanosecond and/or continuous laser beam irradiation [7-9].

For the application of ultrashort pulsed laser irradiation, we employed an ultrashort pulsed laser beam to fabricate an ohmic contact between the metal film and SiC substrate [10]. By irradiating the ultrashort pulsed laser beam from the SiC substrate side, the laser beam could be transmitted through the substrate, reaching the interface between the metal film and the SiC substrate. The irradiated laser beam induced the diffusion of metal atoms into the SiC substrate. In this way, we successfully created an ohmic contact on a SiC substrate at a lower annealing temperature than that of the conventional rapid thermal annealing method [10]. We also applied this concept to fabricate an ohmic contact between a metal contact and a GaN substrate. Our previous study found that Ni atoms, used as metal contacts, did not diffuse into the GaN substrate and failed to form ohmic contacts under any irradiation condition [11]. In contrast, we hypothesized that the GaN substrate acts as an inert window for the metal films on GaN substrates, enabling the formation of a solid solution of Ni and Au, which cannot be achieved under thermal equilibrium on a GaN substrate [11].

High-entropy alloys (HEA) have recently attracted considerable attention. They aim to minimize the Gibbs free energy by moving the edges toward the center of the phase diagram [12]. HEA consist of several elements [13] and are well-known for exhibiting excellent properties such as high yield strength, fracture toughness, and biocompatibility [14]. For the laser processing of HEA, an element map of single-pulse ablation craters of HEA substrates has been reported [13], along with the formation of a laser-induced periodic structure on the HEA substrate [15]. In addition, there have been reports on nanoparticle formation and elemental analysis generated by irradiating the HEA substrate with an Nd: glass femtosecond laser [16]. However, the formation of HEA using ultrashort-pulsed laser irradiation has not been reported. The ultrashort laser pulse induces a non-thermal process after irradiation; thus, it is possible to form novel HEA by ultrashort pulsed laser irradiation.

In this paper, we discuss the pulse duration dependence of the laser-induced alloying of Fe/Cr/Ni metal films on semiconductor substrates. In the Fe/Cr/Ni films, alloying occurs because of atomic diffusion. A longer pulse duration was required to achieve sufficient atomic diffusion. However, a shorter pulse duration was required to alloy novel metals not found in thermal equilibrium. The comparison between these two aspects can be discussed by considering the dependence of metal alloying on the pulse duration.
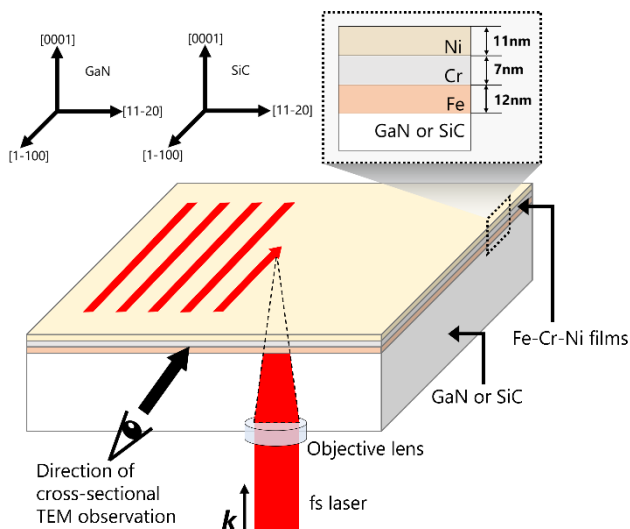
Fig. 1 Femtosecond (fs) laser irradiation and picosecond (ps) laser irradiation were conducted from the substrate side on the interface between substrate and Fe-Cr-Ni-films. For the femtosecond laser irradiation, the scanning lines were parallel to the [1-100] direction of SiC. For the picosecond laser irradiation, the scanning lines were parallel to the [1-100] direction of GaN. The cross-sectional TEM observation was conducted along the laser-irradiated lines.

2. Experimental

We prepared GaN and SiC substrates as transparent semiconductor substrates. The SiC was n-type and its thickness was 350 ± 25 μm. The dopant of n-type SiC was nitrogen with a concentration of 1×10^{15} cm^{-3}. The GaN, 2-μm-thick, was epitaxially grown on a single-crystalline (0001) sapphire wafer, which was 430-μm-thick. The GaN layer consisted of 1-μm-thick undoped and p-type GaN. The dopant

Table 1   Summary of irradiation conditions

Duration	Fluence (J/cm^2)	Scan speed (μm/s)
130 fs	1.01-3.38	25-50
0.65 ps	0.02-0.1	1.5
38 ps	0.02-0.1	1.5

of p-type GaN was magnesium with a concentration of 3×10^{19} cm^{-3}.

Fe, Cr, and Ni films, with thicknesses of 12, 7, and 11 nm, respectively, were deposited on the surfaces of SiC and GaN layers. The Fe and Cr films were deposited under a vacuum pressure lower than 3.15×10^{-6} Pa, using resistance heating evaporation. The Ni film was deposited under a pressure lower than 5.44×10^{-4} Pa vacuum using an electron-beam evaporator.

The source of the femtosecond laser beam was Ti:sapphire regenerative amplifier based on a chirped pulse amplification system (Spectra-Physics Solstice), and that of the picosecond laser beam was a Yb-doped fiber laser. Notably, the picosecond laser beam transmittance for SiC and GaN were 0.26 and 0.84, respectively. Therefore, we used the GaN substrate as an inert window for metal alloying during picosecond laser irradiation.

The details of the femtosecond laser irradiation of SiC are as follows: The wavelength and repetition rate were 800 nm and 1 kHz, respectively. The pulse duration was 130 fs. The laser had a Gaussian energy distribution within the focused spot of diameter 3.07 μm [17]. As shown in Fig. 1, laser irradiation was conducted from the substrate side, focusing on the interface between the Fe film and the substrate. Line patterns were created by moving the stage of the sample at a speed of 25 μm/s, with the laser-irradiated lines spaced
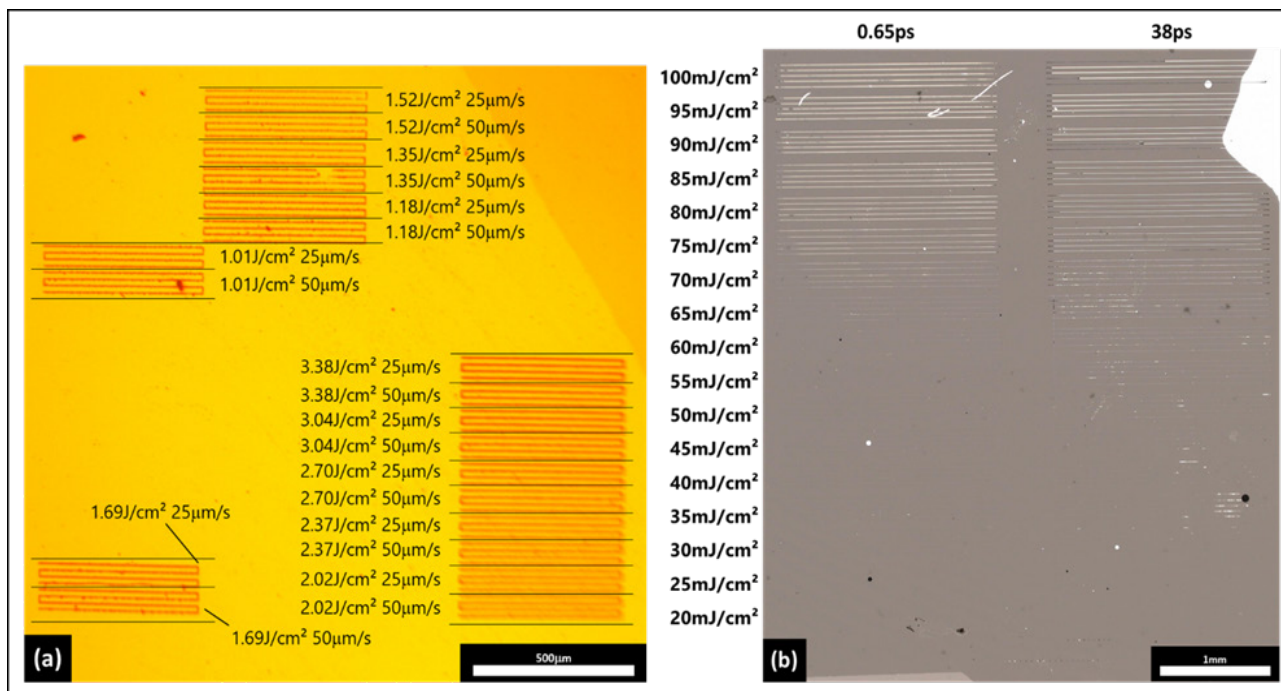
Fig. 2 (a) Optical microscope image of the femtosecond laser-irradiated lines on metal films on SiC. (b) Optical microscope image of the picosecond laser-irradiated lines on metal films on GaN.
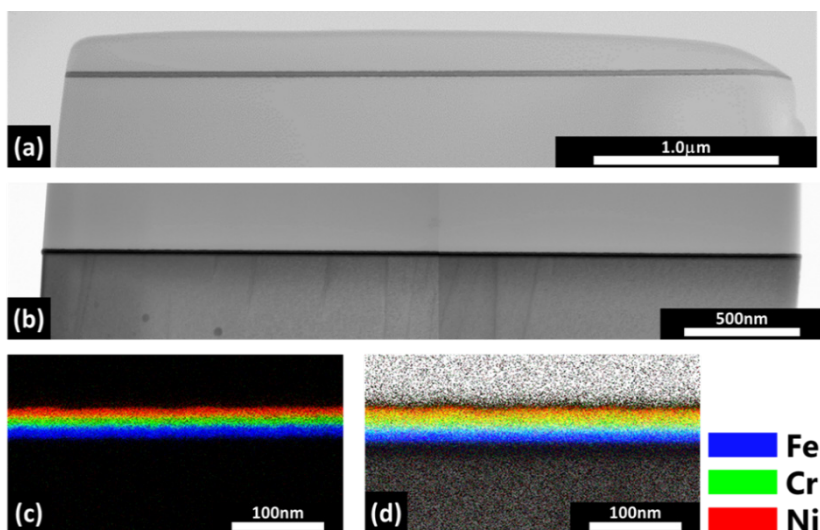
Fig. 3 (a) and (b) are cross-sectional STEM bright-field images of non-modified regions in the metal films on SiC or GaN. (c) and (d) are enlarged images of (a) and (b). The enlarged STEM bright-field images are superimposed by the elemental maps of Fe (blue), Cr (green), and Ni (red).

20 μm apart and running parallel to the [1-100] direction of SiC.

The details of the picosecond laser irradiation of the sample on the GaN substrate are as follows: The wavelength and repetition rate were 1030 nm and 1 MHz, respectively. The pulse duration was 0.65 ps and 38 ps. The focused laser spot had a Gaussian energy distribution and an elliptical shape elongated along the [1-100] direction of GaN. The semi-major and semi-minor axes of the spot were 4.2 μm and 3.1 μm, respectively. As shown in Fig. 1, laser irradiation was conducted from the substrate side by focusing on the interface between the Fe film and substrate. Line patterns were created by moving the sampling stage at a speed of 1.5 μm/s, with the laser-irradiated lines spaced 100 μm apart and running parallel to the [1-100] direction of GaN.

A focused ion beam (FIB) system (JEOL JEM9320FIB) was used to produce thin samples for cross-sectional transmission electron microscopy (TEM) observations. Before the FIB microsampling, a carbon protective film was deposited on the sample surface. The thin samples were lifted off the sample surface using a micromanipulator (Micro Support SS-3FIB-TU). As shown schematically in Fig. 1, cross-sectional TEM observations were conducted along the laser-irradiated lines. Scanning transmission electron microscopy (STEM) images and elemental maps were obtained using a TEM (JEOL JEM-2100F) equipped with an energy dispersive X-ray spectroscopy analyzer.

3. Results and discussion

Figure 2 shows optical microscopy images of the laser-irradiated lines on the metal film surfaces. The irradiation conditions are summarized in Table 1. Fig. 2(a) shows an image of the femtosecond laser-irradiated sample. The laser-modified lines are observed from 1.01 J/cm^2 to 3.38 J/cm^2 for 50 μm/s and 25 μm/s irradiation. Fig. 2(b) shows an optical microscopy image of the picosecond-laser-modified lines on the metal film. Although laser irradiation was carried out from 20 mJ/cm^2 to 100 mJ/cm^2 for 0.65 ps and 38 ps irradiation, laser-modified lines were observed only above 70 mJ/cm^2.

Figures 3(a) and (b) show cross-sectional STEM bright-field images of the non-modified regions in the metal films on SiC or GaN. The metal films in the non-modified regions retained the same morphology as in the as-deposited state. Additionally, the sharp interfaces between the Fe, Cr, and Ni films (Figs. 3(c) and (d)) clearly show that no interdiffusion occurred between the elements.

Figure 4 shows the cross-sectional STEM bright-field images of the laser-modified regions. A bright-field image was captured along the interface between the Fe/Cr/Ni films and
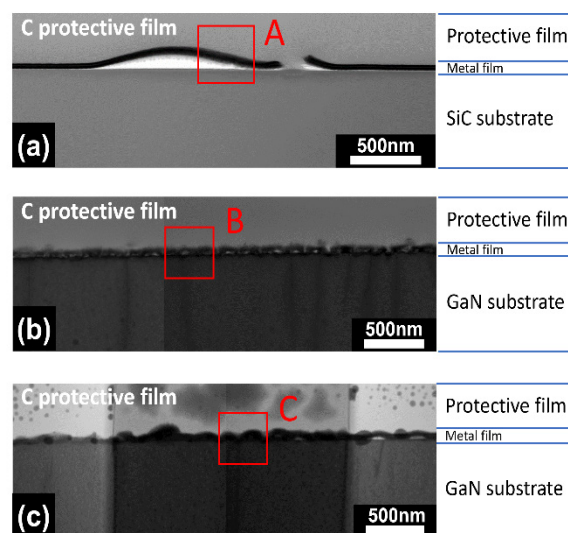
Fig. 4 Cross-sectional STEM bright-field images of laser-modified regions. (a) Laser-modified region irradiated by the femtosecond laser with a pulse duration of 130 fs and fluence of 1.5 J/cm^2. (b) Laser-modified regions irradiated by the picosecond laser with a pulse duration of 0.65 ps and fluence of 0.1 J/cm^2. (c) Laser-modified regions irradiated by the picosecond laser with a pulse duration of 38 ps and fluence of 0.1 J/cm^2.
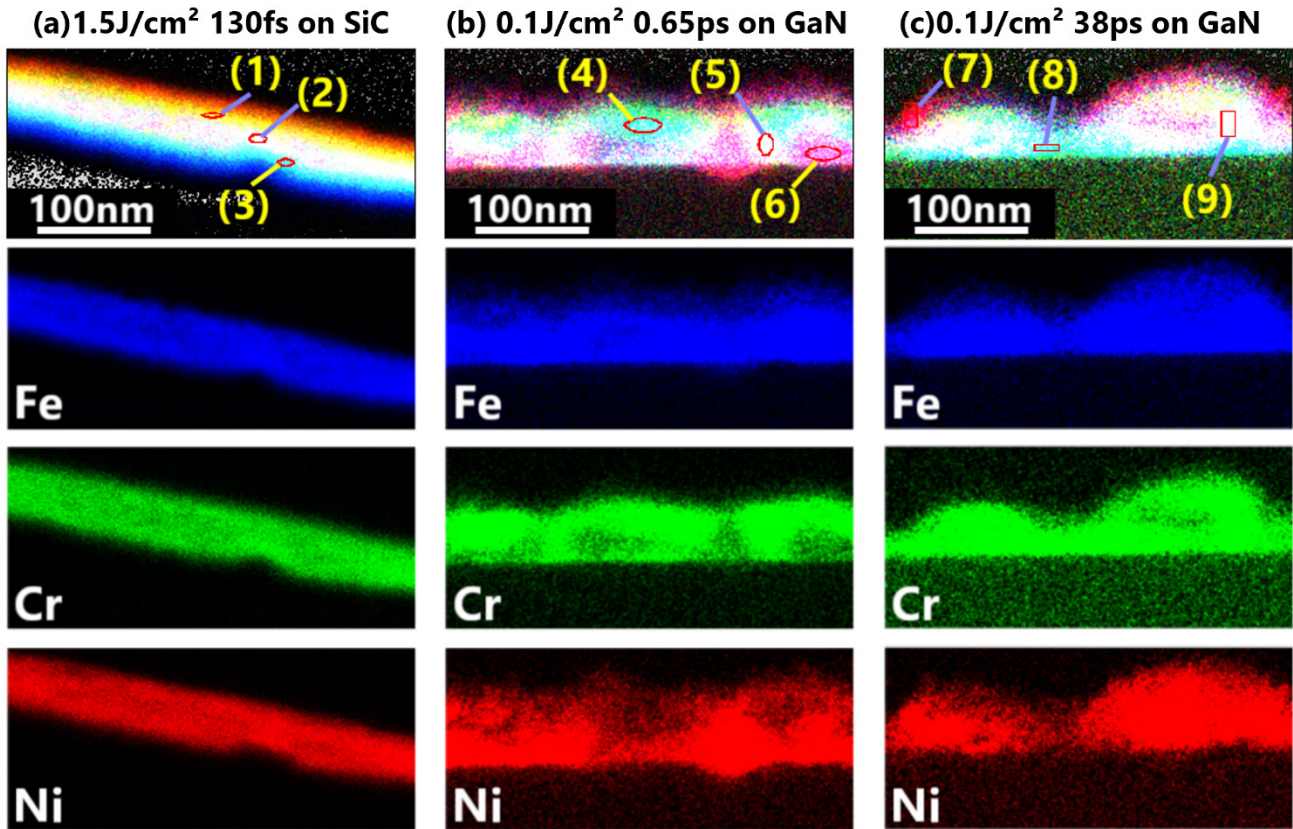
Fig. 5 STEM bright-field image superimposed by element maps of Fe (blue), Cr (green), and Ni (red). (a) Laser-modified region irradiated by the femtosecond laser with a pulse duration of 130 fs and fluence of 1.5 J/cm^2. (b) Laser-modified region irradiated by the picosecond laser with a pulse duration of 0.65 ps and fluence of 0.1 J/cm^2. (c) Laser-modified region irradiated by the picosecond laser with a pulse duration of 38 ps and fluence of 0.1 J/cm^2.

the substrate. The metal film substrate was SiC for 130 fs of irradiation with a peak fluence of 1.5 J/cm^2 (Fig. 4(a)). The metal film substrate was GaN for 0.65 ps irradiation with a peak fluence of 0.1 J/cm^2, and 38 ps irradiation with a peak fluence of 0.1 J/cm^2 (Figs. 4(b) and (c)). Between the SiC or GaN layer and the protective C film, the Fe/Cr/Ni films were present. In Fig. 4(a), a crescent-shaped void was observed between the SiC and metal film. The morphology of the exfoliated metal film showed the Gaussian energy distribution

Table 2 Atomic weight of each atom at different positions.

Area	Fe (atm%)	Cr (atm%)	Ni (atm%)
1	14.70	39.03	46.28
2	39.75	25.63	34.63
3	57.16	32.75	10.09
4	47.81	43.15	9.04
5	45.40	28.15	26.45
6	49.81	13.75	36.45
7	27.14	6.70	66.15
8	47.93	46.47	5.60
9	45.24	27.31	27.45

of the laser. In our previous study, it was reported that exfoliated films produced during laser ablation showed a Gaussian shape [18]. Ablation schemes can be classified into four regimes: vaporization, fragmentation, homogeneous nucleation, and spallation [7-9]. In Fig. 4(a), decomposition into the above four schemes was not observed, indicating that the observed phenomenon was completed before transitioning to the four schemes. It is widely accepted that these four schemes are the initial stages of nonthermal ablation processes. Thus, it was assumed that the phenomena observed in our experiment were related to non-thermal processes. Therefore, further experimental studies are required. The width of the exfoliated area is approximately 1.75 μm. The local fluence at the edge of the exfoliated area was approximately 1.08 J/cm^2 and approximately 0.054 J/cm^2 at the right-hand edge of Fig. 4(a).

As shown in Figs. 4(b) and (c), the interface between the metal films did not exhibit any exfoliation. This was possibly because of the relatively low peak fluence of the picosecond laser beam. In comparison with femtosecond laser irradiation, the interface between the metal film and GaN substrate was rough. This indicates that the entire observed area was modified by picosecond laser irradiation. The protrusions from the GaN substrate side into the metal films are shown in Figs. 4(b) and (c). It is assumed that the roughening of the interface between the metal film and the GaN substrate is caused by explosive ablation due to the local absorption of the laser beam, possibly owing to the impurities in

the GaN substrate. In contrast, the interface between the metal films and the SiC substrate in the region modified by the femtosecond laser was smooth (Fig. 4(a)) owing to the higher crystallinity of the SiC substrate than that of the GaN substrate.

The spatial distributions of the elements in the metal films after laser irradiation are shown in Fig. 5. Figs. 5(a), (b), and (c) show enlarged images of areas A, B, and C, respectively, as seen in Fig. 4. The enlarged bright-field STEM images were superimposed on the elemental maps of Fe (blue), Cr (green), and Ni (red). Areas A, B, and C were close to the center of each laser-modified region.

As shown in Fig. 5(a), (b), and (c), Fe, Cr, and Ni in the femtosecond laser-modified region were mixed more homogeneously than those in the picosecond laser-modified region. This effect was more evident in the Ni distribution, where Ni was mixed more homogeneously in the femtosecond laser-modified region than in the picosecond laser-modified region.

For a more quantitative discussion, the atomic percentages of each constituent element in areas 1 to 9 are summarized in Table 2. From this table, it can be observed that the areas with elemental content less than 15% are 1, 3, 4, 6, 7, and 8. These areas were located in the upper and lower parts of the metal films. In contrast, areas 2, 5, and 9, which lie in the central part of the metal, contained almost the same amounts of the three elements. From this fact, it is assumed that atomic diffusion occurs on the order of 10 nm.

In the following, we discuss the possible relaxation process after femtosecond and picosecond laser irradiation. The experimental results showed that each element was mixed more homogeneously after femtosecond laser irradiation than the picosecond laser irradiation. This implied that the duration of the femtosecond laser pulse was sufficiently long for atomic diffusion. The diffused atoms cooled rapidly and formed a solid solution because of the short duration of the femtosecond laser pulse. Although the duration of a picosecond laser pulse is sufficiently long for atomic diffusion, segregation occurs during the cooling process after laser irradiation. It is assumed that the thermal trajectories after the picosecond laser pulse irradiation follow the pathway in the thermal equilibrium state, leading to segregation according to the phase diagram. At this point, we will measure X-ray diffraction in the near future. Our results show that femtosecond laser irradiation is more suitable for forming novel solid solutions than picosecond laser irradiation.

4. Conclusion

The alloying of Fe, Cr, and Ni on SiC and GaN substrates was discussed. Fe, Cr, and Ni in the femtosecond-laser-modified region were mixed more homogeneously than those in the picosecond-laser-modified region. This effect was more evident in the Ni distribution. In other words, Ni was mixed more homogeneously in the femtosecond laser-modified region than in the picosecond laser-modified region. Although the duration of a picosecond laser pulse is sufficiently long for atomic diffusion, segregation occurs during the cooling process after laser irradiation.

References

[1] D. Bäuerle: "Laser processing and Chemistry" (Springer, Berlin, 2000), 3rd ed. p. 259.

[2] J. E. Sipe, J. F. Young, J. S. Preston, and H. M. van Driel: Phys. Rev. B, 27, (1983) 1141.

[3] J. F. Young, J. S. Preston, H. M. van Driel, and J. E. Sipe: Phys. Rev. B, 27, (1983) 1155.

[4] J. F. Young, J. E. Sipe, and H. M. van Driel: Phys. Rev. B, 30, (1984) 2001.

[5] T. Tomita, K. Kinoshita, S. Matsuo, and S. Hashimoto: Appl. Phys. Lett., 90, (2007) 153115.

[6] J. Reif, O. Varlamova, and F. Costache: Appl. Phys. A, 92, (2008) 1019.

[7] D. Perez and L. J. Lewis: Phys. Rev. B, 67, (2003) 184102.

[8] P. Lorazo, L. J. Lewis, and M. Meunier: Phys. Rev. B, 73, (2006) 134108.

[9] T. Tomita, M. Yamamoto, N. Hasegawa, K. Terakawa, Y. Minami, M. Nishikino, M. Ishino, T. Kaihori, Y. Ochi, T. Kawachi, M. Yamagiwa, and T. Suemoto: Opt. Express, 20, (2012) 29329.

[10] H. Kawakami, Y. Naoi, and T. Tomita: AIP Adv., 8, (2018) 065204.

[11] T. Okada, T. Tomita, H. Katayama, Y. Fuchikami, T. Ueki, H. Hisazawa, and Y. Tanaka: Appl. Phys. A Mater. Sci. Process., 125, (2019) 690.

[12] M. H. Tsai and J. W. Yhe: Mater. Res. Lett., 2 (2014) 107.

[13] D. Redka, C. Gadelmeier, J. Winter, M. Spellauge, C. Eulenkamp, P. Calta, U. Glatzel, J. Mińar, and H. P. Huber: Appl. Surf. Sci., 544, (2021) 148839.

[14] M. Todai, T. Nagase, T. Hori, A. Matsugaki, A. Sekita, and T. Nakano: Scr. Mater., 129, (2017) 65.

[15] D. Zhang, C. Li, J. Xu, R. Liu, R. Duan, K. Feng, and Z. Li: Scr. Mater., 227, (2023) 115276.

[16] F. Waag, Y. Li, A. R. Ziefuß, E. Bertin, M. Kamp, V. Duppel, G. Marzun, L. Kienle, S. Barcikowski, and B. Gökce: RSC Adv., 9 (2019) 18547.

[17] J. M. Liu: Opt. Lett., 7, (1982) 196.

[18] N. Kakimoto, T. Eyama, R. Izutsu, and T. Tomita: J. Laser Micro/Nanoeng., 11 (2016) 91.